LADE: a mobile habitat paving the way for sustained lunar exploration

73rd International Astronautical Congress (IAC), Paris, France, 18-22 September 2022.

IAC-22-A5.1.9.x69560

LADE: A Mobile Habitat Paving the Way for Sustained Lunar Exploration

D. Florenzano*#[a], M. Botti#[b], L. Calogero#[c], A.C.C. Caracas#[d], A. Caruso#[e], C. Chesi[f], M.C. Comparini[g], E. Ferrone[h], J. Hoffman[i], P. Maggiore[j], M. Mattioli#[k], J.A. Paradiso[l], M.A. Perino[m], M. Portolani#[n], A. Rizzo#[o], G. Signorotto#[p], V. Sumini^[q]

[a] *Alta Scuola Politecnica, School of Architecture, Urban Planning and Construction Engineering, Politecnico di Milano, Piazza Leonardo da Vinci 22, Milano 20133*, daniele.florenzano@mail.polimi.it
[b] *Alta Scuola Politecnica, School of Architecture, Urban Planning and Construction Engineering, Politecnico di Milano, Piazza Leonardo da Vinci 22, Milano 20133*, michela.botti@mail.polimi.it
[c] *Alta Scuola Politecnica, Department of Electronics and Telecommunications, Politecnico di Torino, Corso Duca degli Abruzzi 24, Torino 10129,* lorenzo.calogero@studenti.polito.it
[d] *Alta Scuola Politecnica, Department of Structural, Geotechnical and Building Engineering, Politecnico di Torino, Corso Duca degli Abruzzi 24, Torino 10129,* anacarolina.correa@asp-poli.it
[e] *Alta Scuola Politecnica, School of Design, Politecnico di Milano, Piazza Leonardo da Vinci 22, Milano 20133*, alessandro.caruso@mail.polimi.it
[f] *Department of Architecture, Construction Engineering and Built Environment*, *Politecnico di Milano, Piazza Leonardo da Vinci 22, Milano 20133*, claudio.chesi@polimi.it
[g] *Thales Alenia Space Italia, Str. Antica di Collegno 253, Torino 10146,* massimo.comparini@thalesaleniaspace.com
[h] *Thales Alenia Space Italia, Str. Antica di Collegno 253, Torino 10146,* enrico.ferrone@thalesaleniaspace.com
[i] *Department of Aeronautics and Astronautics, MIT, 77 Massachusetts Avenue, Cambridge, USA* jhoffma1@mit.edu
[j] *Department of Mechanical and Aerospace Engineering, Politecnico di Torino, Corso Duca degli Abruzzi 24, Torino 10129,* paolo.maggiore@polito.it
[k] *Alta Scuola Politecnica, School of Architecture, Urban Planning and Construction Engineering, Politecnico di Milano, Piazza Leonardo da Vinci 22, Milano 20133*, marta.mattioli@mail.polimi.it
[l] *Responsive Environments*, *MIT Media Lab, 75 Amherst Street, Cambridge, USA,* joep@media.mit.edu
[m] *Thales Alenia Space Italia, Str. Antica di Collegno 253, Torino 10146,* mariaantonietta.perino@thalesaleniaspace.com
[n] *Alta Scuola Politecnica, Department of Mechanical and Aerospace Engineering, Politecnico di Torino, Corso Duca degli Abruzzi 24, Torino 10129,* marco.portolani@studenti.polito.it
[o] *Alta Scuola Politecnica, School of Industrial and Information Engineering, Politecnico di Milano, Piazza Leonardo da Vinci 22, Milano 20133*, angela.rizzo@mail.polimi.it
[p] *Alta Scuola Politecnica, School of Architecture, Urban Planning and Construction Engineering, Politecnico di Milano, Piazza Leonardo da Vinci 22, Milano 20133*, giulia.signorotto@mail.polimi.it
[q] *Department of Architecture, Construction Engineering and Built Environment, Politecnico di Milano, Piazza Leonardo da Vinci 22, Milano 20133*, valentina.sumini@polimi.it, *Space Exploration Initiative, MIT Media Lab, 75 Amherst Street, Cambridge, USA,* vsumini@mit.edu
* Corresponding Author
# Contributed equally
^ Project Principal Investigator

Abstract

Since Apollo missions, robotic exploration of deep space has seen decades of technological advancement and scientific discoveries. Today, NASA's Artemis Program is envisioning a plan to drive humanity to live on the Moon. Indeed, the possibility of building a permanent settlement on the Moon is still a major challenge. In this framework, Alta Scuola Politecnica and Thales Alenia Space partnered to design a novel agile habitat through a holistic multi-disciplinary approach to allow crewed surface exploration missions.

Lunar Architecture Design Exploration (LADE) project's output is a mobile space architecture system that enables human presence on the Moon, allowing medium to long-term missions. This module is the key movable part to build a more complex system of hybrid class II and class III shelters that aim at the construction of a lunar village.

The goal of the design effort is to allow the permanence of four astronauts on the South Pole of the Moon, next to Shackleton crater. The location is strategic for surface exploration goals and provides favourable environmental conditions for a future permanent settlement. To achieve this, a combination between a mobile habitat and a network of robotically constructed shelters will be necessary. The design of both systems aims at satisfying all habitability and mobility requirements in the harsh and extreme lunar environment while exploiting ISRU, through the demonstration of 3D printing capabilities for micrometeoroids and radiation shielding purposes.

The presence of a sheltering system concurs with a series of minimum infrastructure requirements, which can be reached through a first robotic mission. The aim is to define the first mission elements necessary to sustain a human settlement, including the construction of solid foundations, roads, and landing pads, stabilising the soil, and providing energy production and storage sub-systems.

The iterative process of function allocation within the module and its overall architecture have been guided by the principle of human-centred design. The different mission constraints led to the development of an adaptive system, able to change according to the astronauts' needs and provided with a combination of rigid pre-integrated elements and deployable spaces through pressurization.

The implementation of LADE's functionality into the Artemis mission architecture enables the shift from early exploration phases to a continuous human presence on the lunar surface.
Keywords: mobile space architecture, mobile habitat, shelters, human-centered design, adaptive system

Acronyms/Abbreviations
Lunar Architecture Design Exploration (LADE)
International Space Exploration Coordination Group (ISECG)
Extravehicular activities (EVA)
Galactic Cosmic Rays (GCRs)
Solar Particle Events (SPEs)
Micro-Meteoroids and Orbital Debris (MMOD)
Micro-Meteoroids (MM)
Internal vehicular activities (IVA)
All-Terrain Hex-Limbed Extra-Terrestrial Explorer (ATHLETE)
Japan Aerospace Exploration Agency (JAXA)
Habitat Multivariate Design Model (HMVDM)
On-Line Tool for the Assessment of Radiation in Space (OLTARIS)
Environmental Control and Life Support System (ECLSS)
International Space Station (ISS)
Regenerative Fuel Cells (RCFs)
In Situ Resources Utilization (ISRU)
Benchmark Vehicle (BMV);
Technology Readiness Level (TRL)
Multi-Layer Insulation (MLI)
Lunar Roving Vehicle (RLV)
Master Control Unit (MCU)

1. Introduction

1.1 Context and current mission framework

Lunar Architecture Design Exploration (LADE) is embedded in the principle of human lunar surface exploration. In a global context, according to the International Space Exploration Coordination Group (ISECG) [1], the exploration roadmap is defined in three phases: boots on the moon, expanding and building, sustained lunar opportunities; and six principles: affordability, partnerships, human-robotic partnerships, exploration benefit, capability evolution and interoperability, and robustness.

The first phase (until 2024) is shorter, and its initial capabilities include small cargo landers, gateway, a human lander, extravehicular activities (EVA) hardware and unpressurized rover. The second phase moves toward a sustained lunar presence that includes a focus on mobility, exploration, and science, with a demonstration of pressurized rover capabilities and resource utilization. Lastly, the third one is envisioned as a phase of robust economic activity and development within the lunar environment.

To reach the Lunar Exploration objectives, international efforts have been noted in terms of crewed and robotic missions. Among the crewed lunar exploration and supporting missions, the NASA Artemis program focuses on lunar exploration as preparation for Mars. Three initial missions will lead to a new Moon landing:

- Artemis I (uncrewed system test, 2022),
- Artemis II (crewed mission in cislunar space, 2023),
- Artemis III (crewed Moon landing mission, 2024).

After Artemis III, missions on and around the Moon are proposed to prepare the extension of operations towards Mars (in the 2030s).

LADE fits into this latter phase in which manned exploration missions will be carried out on the Moon and, accordingly, must ensure:

- Reliability of human long-duration habitation capability on the lunar surface;
- Crew health and performance sustainability;
- Independent infrastructure (power and communication systems).

1.2 Mission definition

As part of the efforts to bring humankind successfully to the Moon, and later to Mars, a mission framework must be defined. From a broader perspective, LADE positions itself in the phase of initial lunar exploration, transportation, and exploitation of technology. The project focuses on long-term surface mobility and crew well-being by means of a concept that can allow for long-term explorative human missions.

Indeed, the goal of the project is the design of a mobile habitat unit that can host four astronauts, representing the bridge between the unmanned preparatory missions of lunar site exploration and the effective construction.

Conditions of the Lunar surface

1.2.1 Sources of radiation on the Lunar surface

The space environment determines enormous risks to biological systems and to the performance of materials and devices because of the presence of Galactic Cosmic Rays (GCRs) and Solar Particle Events (SPEs) [2],[3].

The radiation hazard is lower near the poles than in the lower altitude radiation belt, whereas it is more intense in the equatorial region [4]. This is one of the reasons why the region of the South Pole has been proposed as a landing site by NASA Artemis program, an indication used as a reference for the choice of LADE's main outpost location (see *Paragraph 2.1*).

1.2.2 Micro-meteoroids on the Lunar surface

An important observation to be made is that, in the context of lunar surface, the general Micro-Meteoroids and Orbital Debris (MMOD) hazard can be declined in a Micro-Meteoroids (MM) hazard, since orbital debris does not represent a criticality.

The flux of meteoroids represents a significant risk and requires proper protection for critical structures, especially if they are built with light-weight materials [5],[6].

1.2.3 Thermal conditions on the Lunar surface

The Lunar surface exposes vehicles and structures to severe thermal conditions, with a daily temperature difference of approximately 300°C. This is due to the absence of an atmosphere that could absorb heat energy, to the high absorptivity and emissivity, and to the low thermal conductivity and thermal capacity of lunar regolith [7].

2. Mission location and site analysis

2.1 Exploration Goals

Due to the complexity of the lunar harsh environment, the analysis defined in this research is not comprehensive of a full technical-scientific perspective, which would require specific skills and in-depth knowledge. Instead, this paper proposes a method for designing the mobile lunar habitat and its many alternative landing sites, locations of interest and paths to be considered.

This research process begins, as in terrestrial architectural projects, with the identification of possible landing sites and their morphology. Being the project embedded in the Artemis program promoted by NASA, the South Pole (*Fig. 1*) is selected as an area of possible landing site and mission location [8].

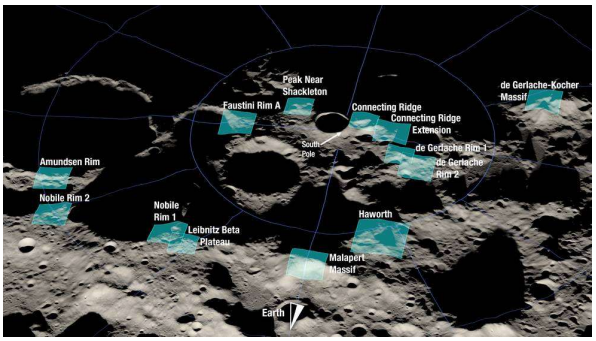

Fig. 1. Landing sites selected by Nasa for Artemis Missions https://www.nasa.gov/press-release/nasa-identifies-candidate-regions-for-landing-next-americans-on-moon (on the right)

The South Pole is not only unexplored and far from the destinations reached by the only astronauts that have ever landed on the Moon during the Apollo missions, it is also interesting due to the presence of ice. With certain areas permanently in the shadow, due to the low inclination of the lunar axis, the environmental conditions contribute to the permanence of ice [9].

2.2 Computational Design: Path Optimization Strategy

Starting from a map depicting the positive (mountains) and negative (craters) altitudes of the Moon's surface, it is possible to extrapolate approximate contour lines that allow the creation of a three-dimensional model of the lunar south pole.

Subsequently, points of interest are selected from mountains and/or craters based on more complete map observations (*Fig.2*).

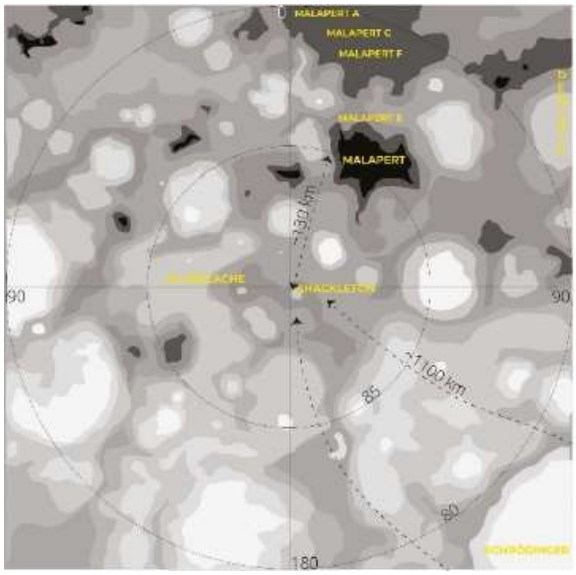

Fig. 2. Topographic map of the Moon's south pole (80°S to pole). Image credit: Lunar and Planetary Institute/Universities Space Research Association/ NASA

A terrain's slopes analysis allows the generation of a map that associates a value of slope to a specific colour. Using a component for mesh creation and analysis (*Bison*) of Grasshopper©, an algorithmic modeling program, it is possible to select only the slope's range of interest, in this case between 0° and 15° constituting the limit values for allowing the designed module to move.

This step highlights that the areas around the craters are extremely steep, beyond the limit values, therefore only a rover is likely to complete the journey in these areas.

The second limitation of the module is represented by the energy autonomy and the radiation protection, which impose a maximum time of 6 hours of self-sufficient movement. The time frame corresponds to a precise distance, depending on the speed of the module and on the inclination of the portion of land crossed.

Two different options have been developed. The first option is to consider the landing point near the Shackleton crater as a place in which the first shelter can be built. Connecting other points of interest and therefore

organizing a network of paths, it gets necessary to subdivide them due to the long distances, identifying the stations for refurbishment.

The *Bison* component is used in union with the evolutionary algorithm of optimization G*alapagos*. Once found the starting and ending points, *Galapagos* identifies the best path through the optimization of values of length and inclination. Then, sub-stations are dislocated along the path, considering energy autonomy.

This option can be considered remarkable in terms of optimization of the path and analysis of slopes along the path, however it is utopic to plan of building a significant number of stops given the amount of time and money to realize them (*Fig.3*).

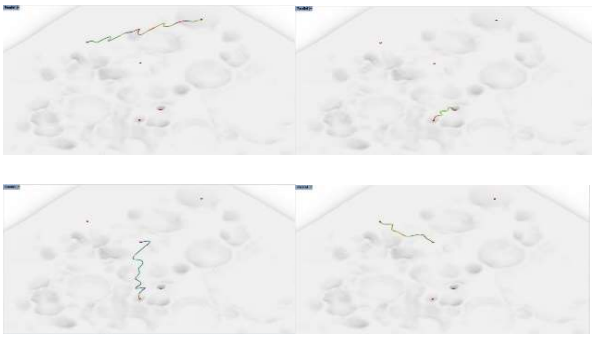

Fig. 3. Paths based on the first strategy proposed

The second strategy is to create a radial development of the mission.

The initial attempt aims at identifying different potential landing sites, as centres of the areas with the lower inclination (almost planar). From them, then, considering the limitations imposed by the autonomy, it's possible to calculate a range of best paths, depending on slope and length. The endpoints of these paths could become the centre of new areas with a maximum radius depending on the position of the sites and on the energetic autonomy of the mobile mdoules.

This strategy is more feasible and it has the advantage of allowing a wide range of explorations without the necessity of building a significant number of stations.

Once the areas of 0° to 5° slope are identified, an average value of speed is assumed. Subsequently, it is possible to get a value of maximal distance considering the 6h time of autonomy.

However, it is discovered that the range of autonomy is much smaller than the size of the concerned areas (0 to 5°). Having all the average values, it is unnecessary to proceed with an optimization of the best path. (Fig.4)

2.3 Results Discussion

Therefore, the result is a network of circles that could be developed to infinity. The radial strategy is a valid one. What is significant through this process is also to discover and experiment with new evolutionary components such as the *Fastloopstart of Anemone* one, that can assimilate the path to a fluid flow. However, paths with both positive and negative inclinations are not considered .

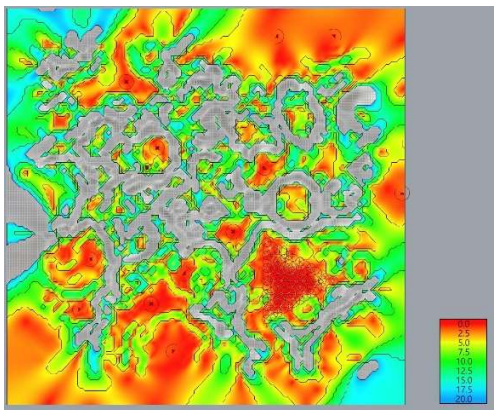

Fig. 4. Radial strategy

3. Material and methods

3.1 Design needs and requirements

Needs and requirements play a crucial role in developing the first layer of priority the LADE mobile modules have to be designed for. Mission requirements establish a fundamental starting point for safe and correct design development. Being a mobile unit, designers and engineers must assure efficient mobility and proper speed for long-distance travel, considering the extreme lunar environmental conditions. In the development phase, it is mandatory to provide enough energy to guarantee self-sufficiency over multiple conditions, adequate shielding, and to allow the conduction of safe routine exploration IVAs and EVAs by the crew members. Consequently, design choices in human missions, as in this project, must deal with redundancy and safety.

Demonstrations of the reliability of human long-duration capability and operational procedures on the lunar surface, alongside the ability to develop the infrastructure necessary to achieve the objectives for sustained exploration, are necessary to define the number of crew members and mission duration. In particular, four astronauts and a maximum of six hours long missions are determined.

Human spaceflight necessitates more than only technical requirements. Indeed, preserving the safety of the crew also means providing the mandatory functions to sustain the crew from physiological and psychological well-being. Every moment of the mission is therefore defined and translated into a design decision.

Furthermore, science, logistics, and maintenance operations require specific tools and spaces inside the module to make the crew able to fulfill sample collection, analyses, prioritization, and storage, alongside

maintaining the exploration asset during recognized maintenance intervals.

3.2 Literature review

Several case studies are analysed during the concept development and play a determining role in defining a solid literature background for complex decision-making processes. The construction of a fitness matrix of case studies allows the comparison of different adopted solutions contributing to comprehending the pros and cons of each decision. The results are synthesized in *Table 1*, in which the features and subsystems of the selected case studies are assessed on a scale from 1 to 3 considering the general efficiency of the categories of radiation shielding, energy supply, mobility system, speed constraints, modularity, and mission duration.

Table 1. Fitness matrix of case studies

	JAXA	LER	Scorpion	Habot
Radiation shielding	/	/	⋆⋆⋆	⋆⋆⋆
Energy supply	⋆⋆⋆	/	⋆⋆	⋆⋆
Mobility system	⋆⋆⋆	⋆⋆⋆	⋆⋆⋆	⋆
Speed constraints	⋆⋆⋆	⋆⋆	⋆⋆	⋆
Modularity	/	/	⋆⋆⋆	⋆⋆⋆
Mission duration	⋆	⋆⋆⋆	⋆⋆	⋆⋆⋆

These projects present interesting and reliable design references regarding the mobility system and the number of wheels, from the ATHLETE used in Habot [10], which presents the critical ability to reach high speed, to a more sophisticated system of foldable legs as in the Scorpion [11], reaching technologies present in Mars rovers like the rocker-bogie structure. Optimal design output is reached by the JAXA module [12] for its interesting use of hydrogen fuel cells in addition to the more traditional deployable solar panel system. Moreover, Habot represents an optimal example of Habitat Multivariate Design Model (HMVDM), to estimate volume, size, shape, and configuration required for the design of a space habitat and its crew [13].

3.3 Concept idea

Focusing on the goal of performing medium to long-term explorative crewed missions on the Moon's surface, LADE project envisions a network of shelters in support of different mobile modules that allow research and explorative missions over significant distances.

The presence of the settlements of hybrid class II and class III is essential to guarantee thermal and radiation protection to the crew and the equipment in the considered mission duration, maximizing ISRU. Moreover, they perform the indispensable role of providing power supply, storage for maintenance equipment, and life support essentials like food production facilities, water production, waste management. They also host pressurized crew cabins with sleeping areas and personal spaces to also guarantee the psychological well-being of the astronauts.

The design of pressurized mobile modules enables crewed missions lasting up to 6 hours from the reference shelter. LADE project envisions a typology of mobile modules which answers to a wide range of mission goals and requirements because of differences in their functions and internal distribution. The concept idea is to provide a range of mobile modules, joinable through airlocks, to choose from to perform a specific mission.

LADE project is born from deep analysis and, afterward, interpretation of bees. The natural reference is reshaped into a futuristic vision of a lunar swarm and its hive. The project envisions the shelters and the mobile modules as strictly dependent elements reciprocally essential to be and to work.

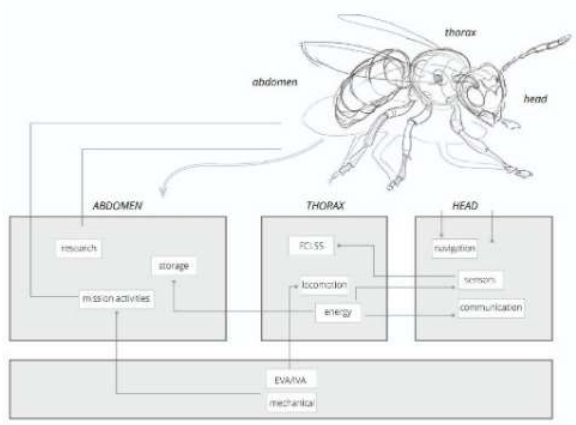

Fig. 5. The biophilic approach visible in the functional distribution of the mobile modules

The biophilic approach (*Figure 5)* is used also in the design of mobile modules whose functional distribution

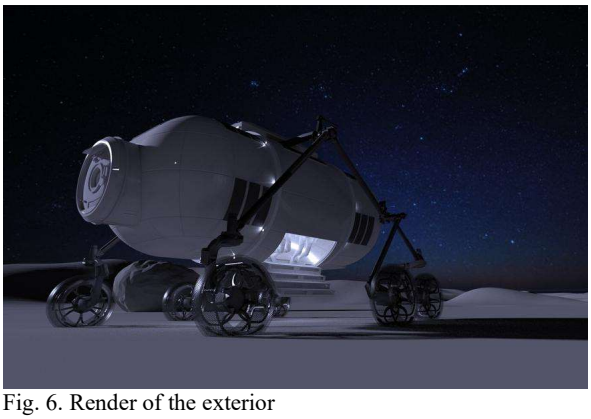

Fig. 6. Render of the exterior

is inspired by the bee's body. When connected they resemble the head, the thorax, and the abdomen of the considered animal by their functions: navigation, communication, locomotion technologies, and EVA system in the primary module, and research or storage in the secondary one.

Following the same reference, the selected technique of traveling of the mobile modules resembles the swarm of bees in terms of the constitution of a group of single units moving in the same directions and working on the same scope. To guarantee a specific order and to minimize the space for navigation tools and control equipment in the mobile modules, the project envisions the presence of a primary mobile module in charge of

Fig. 7. Render of the exterior

navigating and paving the way, followed through computer vision, AI, and fleet learning by the secondary modules selected for the mission, each of them provided by their own mobility system.

This technology enables significant flexibility of the desired performances according to the mission.

The currently designed modules are the primary one for navigation and control and the secondary ones dedicated to research, storage, or transportation. The focus of the LADE project so far has been the mobile modules.

4. Subsystems

4.1.1 Structure

4.1.1 Geometry composition

The geometry of the module has been constrained by the current technological and volumetric constraints required for the payload launch from Earth and the current limitation of the launcher's capabilities according to the Artemis Missions framework. The selected launcher for the specific mission is the SLS Block 1B Cargo, which allows for 8,4 m diameter Fairing Class and a mass payload limit of 37-40tons, but the design of the structure of the system and its deployment sequence has been constrained to the Fairing limitations of the smaller SLS Block 1 Cargo, with a 5m Fairing Class and a mass payload limit of 26tons [14]. The geometry of the shell has been therefore designed as a simil-cylindrical shape, the section of which is inscribed within a circle of 4.5 m in diameter. The organization of the structural system for the primary module has been defined based on the functional needs and the payload constraints described in Paragraph 4.1.1. For the purpose of this paper, the complexity of the structural system for a mobile lunar habitat, which presents an extended series of load bearing components divided into primary and secondary structures [15], has been simplified into two main macro-elements: the independent structure of the mobility system, which includes the structural elements composing the modified rocker-bogie mobility system supporting the structure of the shell, and the shell structure itself containing the pressurized habitat space. A quasi-identical configuration has been adopted for the secondary module. These two macro-elements are separable to allow for a greater reduction in payload volume and increase the replacement capabilities in case of malfunctioning of a specific subsystem.

The structural system sustaining the rocker-bogie is planned to land on the lunar surface as a separate deployable element, composed of a series of telescopic structural arms joining the main structural frame, containing the differential and the surface to 3 pairs of Nitinol wheels [16] selected for the mission.

The shell structure, on the other hand, is composed of a panel structure reinforced by a network of lightweight beams in the most stressed areas. Structural optimization was performed to define the most efficient configuration of sections of both beam and shell elements. The panel structure of the shell has been subdivided into two main elements: the pressurized shell, which has the role of resisting working pressurization loads and the reduced gravity of 1,62 m/s^2, and an exterior central segment which addresses the challenge of protecting the suitports and the relative spacesuits from the highly abrasive lunar regolith, while serving as a support for the entrance and exit of astronauts from the vehicle during EVA.

4.1.2 Tools to analyze structural elements

This work has been analyzed and optimized through computational methodologies of the shell structure of the primary LADE module, the geometry of which has been completely developed within Grasshopper [17]. In particular, the structural analysis has been performed with the Grasshopper plug-in Karamba3D® [18].

4.1.3 Definition of structural principles

a. Environmental considerations

When designing a structure that is meant to be operated in space, it is necessary to consider multiple loading conditions affecting the structure in different mission phases. Severe vibrations and dynamic loads during launch, initial flight phase, descent and landing could be

encountered by the designed structure, to the extent that these loads could be more critical than the operational loads. Another important aspect to be considered is the Moon's gravity, which accounts for roughly 1/6 of Earth's gravity, impacting the calculations for structural dead loads. Another factor to be accounted for is the lack of a consistent atmosphere, making necessary the pressurization of the interior spaces to 1 atm, creating an outward directed load on the whole pressurized surface of the shell. Along with these considerations, another crucial aspect from a structural standpoint is the exposure to extremely harsh temperature excursions, which could impose a heavy thermal loading condition on the structures [19].

The goal of the structural analysis was to perform a simple static analysis of the shell structure to optimize the sections of the shell and guide the conceptual design of the module through an informed approach. Further research would require performing a dynamic analysis of the structure and a modal analysis of structural vibration both in launch and operating condition (motion on the surface) to further validate the shape designed.

b. Material consideration

Due to the correlation between structural macro elements and their different requirements from a structural point of view, different materials have been considered for the structure of the rocker-bogie and the shell. For the first one, as the structure is required to sustain both its own weight and the one of the shell, a high-performance titanium alloy, Ti-5AI-5V-5Mo-3Cr, developed for the utilization in aircraft landing gears, has been selected [20].

For the shell structure, which is required to sustain the pressurization load of the interior spaces of the module and its own weight, a lighter Al-Li alloy, AA2060-T8, has been selected to reduce the burden on the mobility system [21]. An additional material, the borosilicate glass, has been selected for the transparent portions of the shell, due to its high resistance to thermal shock and its optimal mechanical properties for space uses [22]. *Tab.2* provides information on the mechanical properties of the three materials considered.

Table 2. Mechanical properties of structural material

Element	Material	Young's modulus [GPa]	Tensile strength [MP]	Compressive strength [MPa]	Poissn ratio
Rocker-bogie	Ti-5Al-5V-5Mo-3Cr	110	1244.5	1265.2	0.29
External shell	Al-Li alloy AA2060-T8	76.5	476	470	0.33
Glass window module	Borosilicate Glass	64	81.6	914.7	0.20

c. Geometrical considerations

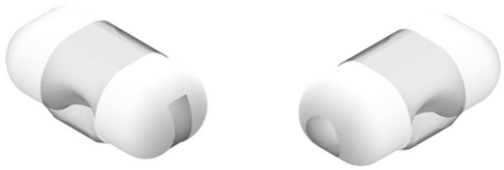

Fig. 8. The shell obtained from a parametric model

A series of requirements have been considered while designing the structure of the shell of the module. First of all, due to the particular conformation of the rocker-bogie mobility system [23], which requires the positioning of the differential and the main axis in alignment with the center of mass of the structure, making it more efficient to opt for a symmetrical structure [24].

Another geometrical consideration has been made towards the avoidance of sharp edges in the structure,

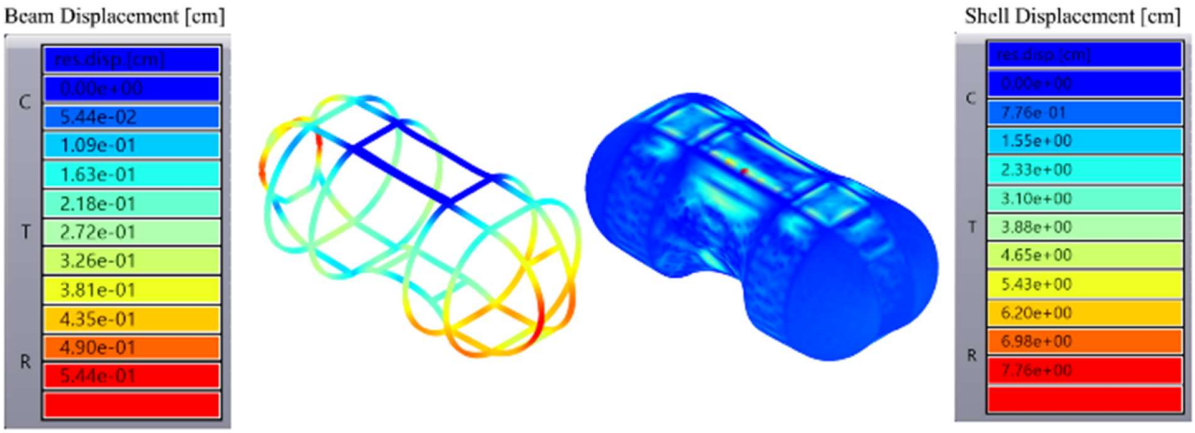

Fig. 9. Grade of Displacement occurring on beam and shell structure

selecting curvilinear and cylindrical shapes to reduce stress concentration and improve the manufacturability of the structure.

The resulting geometry is therefore composed by 3 portions, which include a central segment, symmetrical with respect to the center of mass of the structure, and curved inwards to allow space between the inner pressurized shell and the external one to store the space suits within the shell, and two quasi hemispherical shells which host on one side the airlock dedicated to the physical connection with the secondary module and on the other one the opening in correspondence with the navigation cockpit. These three segments are connected between each other by a transition segment with a cross section composed by two half circular arches and two horizontal beams, in order to expand the horizontal floor surface of the module and increase the usable interior space for the astronauts. Figure 8 shows the parametrically modelled geometry of the shell.

4.1.4 Optimization/Computational design workflow

The analysis and optimization of the structure of the pressurized shell performed in Karamba3D has allowed to inform the design choices for the module. To achieve this, the computational design workflow that has been followed includes a series of steps as described below.

First of all, modelling of the shell structure, which included the integration of the cockpit opening and the airlock opening. The Rhinoceros® [25] native NURBS [26] geometry has been then transformed into a mesh of variable density to be compatible with the Karamba3D environment.

Secondly, setting up of structural model. This step included the definition of the loads applied to the structure and the load combinations, as well as the supports sustaining the structural elements (i.e. the connections with the rocker-bogie structure, transforming the whole shell into a hanging system due to the connection through mechanical clamping) and the cross sections for both the structural panels and the supporting light beams defined in Paragraph 4.1.1. The applied loads include gravity load, the operation pressurization load of 1 atm, and an additional mesh load constraint to consider the loading of the permanent elements of the structure, in particular the shielding elements and the batteries, which together account for approximately 6700kg of mass. The beam structure sections have been associated with hollow square beams with a 10cm side and a thickness of 1.2cm, whereas the sections selected for the shells is variable as it is the object of optimization. Both structural elements have been applied the same Al-Li alloy as described in Paragraph 4.1.3.

Lastly, the analysis of shell and beam sections was conducted. The analysis produced a series of graphic outputs where the stresses and displacements are detected. In particular, the two aspects that have been considered were the displacements and the section utilizations of both the shell and the beam structure. *Fig. 9* shows displacements occurring on the beam and shell structure, in which can be noticed the presence of maximum displacement in correspondence of the cockpit opening. It is important to mention that in this simulation the presence of the collaborative effect of the borosilicate glass window is not accounted for. Another important aspect to be considered is the higher displacement recorded in the upper central area of the shell, in the vicinity of the supports.

Looking at *Fig. 10*, the spherical structures at both ends of the structure experienced uneven distribution of section utilization, with a reduced value for the spherical elements. Overall, the displacement and section utilization diagrams show a comparable behavior.

4.1.5 Structural optimization and design choices

The structural analysis of the pressurized shell has uncovered the necessity to adapt the structural sections to the different displacement and stress conditions to obtain

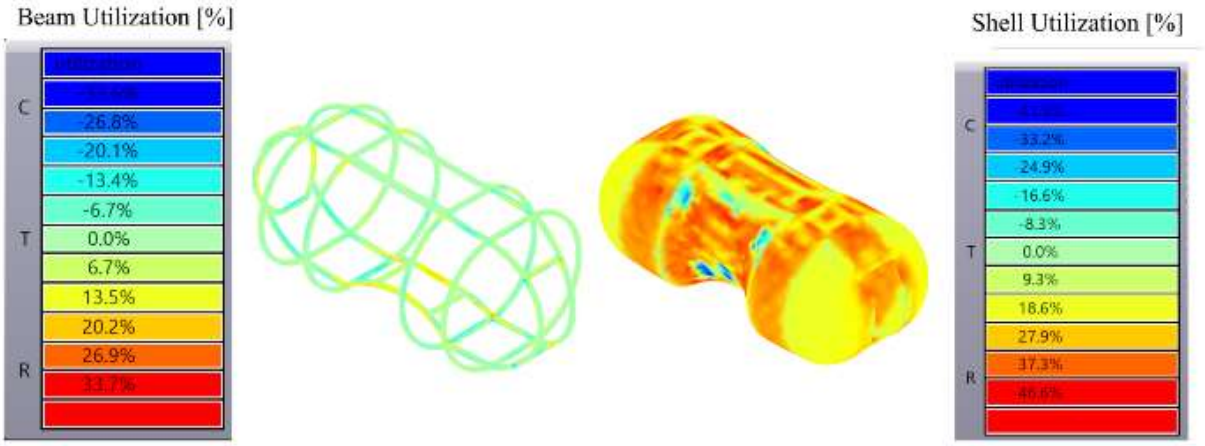

Fig. 10. Section Utilization on the beam and shell structure

a more evenly distributed response of the structural system to the applied loads.
In particular two actions have been undertaken to improve the structural performance: first, additional segments of supporting light beams have been introduced in highly stressed areas, then the shell portions that presented maximum displacement and with the highest section utilization have been modified increasing the shell's thickness by a factor of two, going from the initial 1.25 cm of the first analysis, to a double layer panel of 2.50 cm.

4.2 Locomotion system

The choice of the locomotion system is a crucial step in the design of the mobile habitat. The module should be able to move reliably and dexterously on the harsh lunar surface, ensuring: a high robustness to possible failures; the capability to traverse obstacles having sizes comparable to the moving elements of the locomotion system; the ability to climb slopes within the range of the most frequent inclination angles of the Moon's surface.

4.2.1 Comparison of locomotion systems

Three main locomotion systems can be used for the mobile habitat:

- Wheel-based system;
- Track-based system;
- Rocker-bogie system.

To choose which of these systems is the most suitable one for the mobile habitat, a comparison between them must be carried out, focusing on the aspects of mobility performance, reliability, energy consumption, obstacle traversing, and TRL.

To comprehensively compare the locomotion systems, experimental or simulation data, based on operations in planetary terrain-like environments, is required. Such data, however, is scarce in literature and the existing studies focus only on exploration rovers, rather than proper mobile habitats.

Therefore, the comparison of the three locomotion systems is carried out qualitatively, by evaluating the major strengths and weaknesses of each system by means of different "metrics", which are qualitative parameters reflecting the general performance of one aspect of the vehicle.

To each metric is assigned a grade, corresponding to how the locomotion system performs well on that specific metric: from ⋆ (i.e. 1 star) to ⋆⋆⋆⋆⋆ (i.e. 5 stars).

The metrics that are used to evaluate each locomotion system can be found in *Table 3*.

The grades for each metric are then quantified by means of a fictional locomotion system, denoted as a "benchmark vehicle" (BMV). The metrics of the BMV are associated with the middle grade (⋆⋆⋆) and each of them is provided with a quantitative value, which corresponds to the ideal requirement for LADE mobile habitat on that specific metric. These values can be easily extended to the other grades of each metric.

The BMV metrics are then compared with those of the three locomotion systems of interest (*Table 4*).

Table 3. Comparison criteria and grades

Metrics	⋆	⋆⋆	⋆⋆⋆ **(BMV)**	⋆⋆⋆⋆	⋆⋆⋆⋆⋆
Maximum speed	< 5 km/h	up to 5 km/h	10 km/h	up to 15 km/h	> 15 km/h
Obstacle traverse	< 50%	50%-75%	Moving elem. size (100%)	100%-125%	> 125%
Slope climb	< 10°	up to 10°	15°	up to 20°	> 20°
Soil sinkage	very high	high	-	low	very low
Mechanical simplicity	very low	low	-	high	very high
Mobile element redundancy	no redun-dancy	low	-	high	very high
Energy consumption	very high	high	-	low	very low
Payload mass fraction	< 25%	25% - 50%	50%	50% - 75%	> 75%
Soil interaction	very high	high	-	low	very low
TRL	TRL 1-2	TRL 3-4	TRL 5	TRL 6-7	TRL 8-9

Table 4. Results of the comparison

Metrics	**Wheel-based system**	**Track-based system**	**Rocker-bogie system**
Maximum speed	⋆⋆⋆⋆⋆	⋆⋆⋆⋆⋆	⋆⋆⋆
Obstacle traverse	⋆⋆	⋆⋆⋆	⋆⋆⋆⋆⋆
Slope climb	⋆⋆	⋆⋆⋆	⋆⋆⋆⋆
Soil sinkage	⋆⋆⋆	⋆⋆⋆⋆⋆	⋆⋆⋆⋆
Mechanical simplicity	⋆⋆⋆	⋆⋆	⋆⋆
Mobile element redundancy	⋆⋆⋆⋆	⋆	⋆⋆⋆⋆
Energy consumption	⋆⋆⋆⋆	⋆⋆	⋆⋆⋆⋆
Payload mass fraction	⋆⋆⋆	⋆⋆⋆	⋆⋆⋆
Soil interaction	⋆⋆⋆	⋆	⋆⋆⋆
TRL	⋆⋆⋆⋆⋆	⋆⋆⋆	⋆

4.2.2 Choice of locomotion system

Given the comparison from *Paragraph 4.2.1*, the most significant metrics, for the purposes of LADE mobile habitat, are obstacle traverse and slope climb capabilities, mobile element redundancy, and soil interaction. With reference to *Table 4*, the locomotion system that scores the best results in these metrics is the rocker-bogie system.

4.2.3 Thrust of the locomotion system

The rocker-bogie is a 6-wheel locomotion system topology; therefore, thrust is provided by 6 in-wheel brushless DC motors. The lack of brushes and, in general, the absence of any mechanical part visible from the outside ensures higher robustness to failure of the locomotion system, due to infiltrations of regolith and other abrasive materials in the wheels. Moreover, DC motors allow to directly use the electrical power coming from the battery, with the need of only DC-DC converters (which are light, compact, and resilient) instead of transformers (which are heavy, bulky, and more fragile).

The motors are separately controlled by the onboard Master Control Unit (MCU). Using a conventional steering system (i.e., the 2 front wheels of the rocker-bogie are active steering wheels), the motors speeds are regulated by an electric differential while making turns. The steering wheels are actuated by 2 steering DC motors.

4.2.4 Rocker-bogie wheels

As previously mentioned, the variety of lunar terrains requires the ability to cross different surfaces, such as steep rocky slopes or wide sand dunes, and makes it impractical to use ordinary wheels for terrestrial applications. By analyzing the solutions adopted in the latest generation of rovers and new studies on innovative materials and technologies, two different configurations that fully reflect the philosophy of seeking innovation inherent in the entire project are considered [27]:

- Reconfigurable wheel-track developed by DARPA and Carnegie Mellon University's National Robotics Engineering Center, consisting in a mechanism that can transition from a round wheel to a triangular track. They ensure faster travel in a range of terrains and a high load-bearing capacity [28].
- Superelastic tires by NASA Glenn, non-pneumatic, compliant tire utilizing shape memory alloys (mainly Nitinol) as load-bearing components. It is a strong, robust and lightweight solution which can withstand excessive deformation and offer high traction on various terrains [29],[30].

Because of the many critical aspects presented by the reconfigurable wheel, primarily mechanical complexity, weight, and incompatibility with lunar regolith, the choice for the LADE module fell on superelastic tires.

4.2.5 Wheel sizing

A first wheel sizing derives from the study of vehicle trafficability in the case of soft terrain, exploiting the wheel sinking and the drawbar pull, i.e., the difference between traction and movement resistance. The procedure, the equations and the parameters needed to derive the wheels' diameter and width come from [31].

Considering a preliminary and approximated mass of 12 tons, the module needs 6 wheels with a diameter of 1.5m and a width of 0.6m.

4.3 Shielding

To ensure the safety of the astronauts, the proposed shielding combines three kinds of protection: from radiations, micrometeoroids, and harsh temperature variations.

4.3.1 Radiation shielding

The proposed radiation shielding aims at limiting the hazards derived from exposure to GCRs. Indeed, it is envisioned to achieve adequate protection from SPEs by providing appropriately designed shelters (*Paragraph 3.3*).

Instead of traditional Aluminum, novel hydrogen-based materials are currently studied for their advantageous properties (lower secondary radiations, stronger fragmentation effect, and low density) [32],[33]:

- Polyethylene (PE).
- Low-density complex hydrides, such as $^{6}Li^{10}BH_4$, ^{6}LiH, and NH_3BH_3.
- Intermediate-density composites, such as graphene oxide (GO) nanoplatelets reinforced plastics (1% wt GO, 2 % wt GO and 5% wt GO).

All these materials proved excellent shielding capabilities in terms of radiation dose reduction, in comparison with Aluminum and also with other polymers (i.e., PEEK, PPS, and Kapton).

From the literature analysis, the materials that emerge as the best candidates for radiation shielding are MDPE (Medium Density Polyethylene), ^{6}LiH, and MDPE reinforced with 5% wt GO (Graphene Oxide).

4.3.2 Micrometeoroids shielding

The choice of the materials and the configuration for the layer of MM shielding is guided by reference configurations obtained from papers and already existing modules [3], [34]. In these studies, Kevlar and Nextel fabrics are the most frequently used materials [35],[36].

These materials allow the achievement of two possible configurations: the stuffed-whipple one and the multi-shock one [6]. The most suitable MM shielding should be a multi-layered and multi-shock one that, from the outermost to the innermost layer, consists of multiple alternate layers of Nextel (4 layers) and Kevlar (17 layers), followed by a rear layer of Aluminum.

The MM shielding layer has to be uncoupled from the innermost layers, in order not to damage, in case of impact, the pressurized portion of the module. Therefore, spacers have to be provided, in the form of Polyimide AC550 (now SOLIMIDE®) open-cell foam [34].

4.3.3 Thermal shielding

Multi-Layer Insulation (MLI) is a type of high-performance thermal insulation which is the most frequently used in aerospace applications. Consequently, the standard ISS MLI design [37] is proposed for the

module. It is composed of a Beta Cloth outer layer and 10 alternate layers of Kapton (Single Aluminized Polyimide, SAP) and Mylar (Double Aluminized Polyimide, DAP). Furthermore, the individual layers are separated by a Dacron netting (spacers) to minimize conductive heat transfer between them.

4.3.4 Dimensioning of the shielding

As far as it concerns the micro-meteorites and thermal shielding, average thicknesses found in the previously mentioned case studies and papers are proposed for the module.

As to the radiation shielding, instead, given the novelty of the proposed materials, simulations with NASA's software OLTARIS© [38], [39] are conducted to determine the optimal configuration. The three selected materials for the radiation shielding are the ones highlighted at the end of *Paragraph 4.3.1*.

The following parameters are selected for the simulations:

- Environment: GCR, Free Space 1UA;
- Historical min/max: 2011 Solar Min (worst-case scenario);
- Mission duration: 1 day;
- Geometry: User-defined Slab (semi-finished plane);
- Dose: measured in Tissue;
- Dose Equivalent (solid cancer): quality factor NASA Q.

The equivalent dose limit set by NASA for astronauts is 50 REMs per year, or 0.5 Sv [40]. This limit is equivalent to a maximum equivalent dose of 1.37 mSv per day. Considering a very conservative margin of 10%, astronauts in the module cannot exceed a maximum dose of 1.23 mSv per day.

In all the simulations, the order in which materials are described is from the outermost to the innermost.

First, proof-of-concept simulations (with thicknesses that do not provide the envisioned protection from radiations) are run to decide which could be the best order to arrange materials. In all the configurations, a total thickness of 4 cm is considered for the overall radiation shielding. Then six simulations are run: A1, A2, A3, B1, B2, and B3.

To determine the materials and the orders that provide the best efficiency in shielding GCRs radiations, A1 simulations with three monolayers, A2 simulations with configurations of two materials, and A3 simulations with configurations of three materials are run.

From the results of the A1 simulations, it emerges that MDPE_GO is the material providing the greatest efficiency in shielding GCR radiations, followed by LiH and MDPE. As a consequence, in configurations with two layers, the combinations that do not present MDPE_GO are excluded.

From the results of the A2 and A3 simulations, it emerges that the configurations in which MDPE_GO is the innermost material are the most efficient ones.

Once assessed the most efficient order of materials, overall simulations with three, two, and one layer (B3, B2, and B1 respectively) are conducted. To take into account all the layers presented in the proposed shielding, multilayer configurations with also MM and thermal shielding are considered in the simulation. Dacron netting, Polyimide foam, and Beta Cloth are excluded from the analysis.

From the results of B1, B2, and B3 simulations (*Tables 5-7*) it emerges that the solution that allows the most efficient trade-off between the shielding capability and the overall mass of the shielding structure is B1.3e. Indeed, this configuration allows for a reduction of the equivalent dose up to 1.1990 mSv/day and an overall mass of 5758.00 kg.

Table 5. Results of OLTARIS B3 simulations

Case	Description	Equivalent dose [mSv/day]	Mass [kg]
B3.21a	MDPE 1cm + LiH 1.5cm + MDPE_GO 1.5cm	1.3639	5443.00
B3.21b	MDPE 1.5cm + LiH 1cm + MDPE_GO 1.5cm	1.3769	5523.00
B3.21c	MDPE 0.5cm + LiH 1.5cm + MDPE_GO 2cm	1.3182	5458.00
B3.21d	MDPE 1.5cm + LiH 0.5cm + MDPE_GO 2cm	1.3434	5618.00
B3.21e	MDPE 1.5cm + LiH 0.5cm + MDPE_GO 3cm	1.2613	5648.00

Table 6. Results of OLTARIS B2 simulations

Case	Description	Equivalent dose [mSv/day]	Mass [kg]
B2.23a	MDPE 2cm + MDPE_GO 2cm	1.3558	5698.00
B2.23b	MDPE 3cm + MDPE_GO 1cm	1.4521	5668.00
B2.23c	MDPE 1cm + MDPE_GO 3cm	1.2727	5728.00
B2.13a	LiH 2cm + MDPE_GO 2cm	1.3054	5378.00
B2.13b	LiH 3cm + MDPE_GO 1cm	1.3702	5188.00
B2.13c	LiH 1cm + MDPE_GO 3cm	1.2491	5568.00

Table 7. Results of OLTARIS B1 simulations

Case	Description	Equivalent dose [mSv/day]	Mass [kg]
B1.3a	MDPE_GO 3cm	1.3557	4788.00
B1.3b	MDPE_GO 3.25cm	1.3169	5030.50
B1.3c	MDPE_GO 3.50cm	1.2754	5273.00
B1.3d	MDPE_GO 3.75cm	1.2362	5515.50
B1.3e	MDPE_GO 4cm	1.1990	5758.00

In conclusion, the proposed shielding configuration is summarized in *Table 8*.

Table 8. Complete configuration of the shielding of the module (from the outermost to the innermost layer: thermal, micrometeoroids, and radiation shielding)

Material	Density [g/cm^3]	Thickness [cm]	Shielding
MDPE_GO	0.9725	4.000	*Radiation*
Aluminium	2.7	0.259	*MM*
Kevlar (x17)	1.44	0.243	*MM*
Nextel (x4)	2.79	0.147	*MM*
Polymide foam	0.0071	2.535	*Spacing*
Dacron netting	0.0063	0.159	*Thermal*
Kapton (x10)	1.33	0.143	*Thermal*
Mylar (x10)	1.39	0.144	*Thermal*
Beta Cloth	0.015	0.600	*Thermal*

4.4 Power subsystem

4.4.1 Power and mass budget

To define the power requirements of the primary module, a general analysis of each of its functions, both in terms of power and mass, is carried out. The results are summarized in *Table 9*, considering references from the literature [41]–[44].

Table 9. Power requirements and mass analysis of the primary module

Function	Power [W]	Mass [kg]
Navigation and control	180	165
ECLSS	650	1346
Waste management	3	122
Communication	200	35
EVA support	300	375
Storage	0	50
Communication with the other module	0	200
Power system	0	958
Mobility	5400	1817
Interiors	89	330
Structure	0	700
Shielding	0	5700
Total	6822	11798

A detailed energy budget is proposed to determine the energy that have to be provided to the mobile module, considering the hourly consumption for two six-hours missions.

- Mission A (primary module + laboratory secondary module): two-hours travel from a shelter to a spot of interest, two-hours operations (sample collection and laboratory activities), two-hours travel back to the shelter.
- Mission B (primary module + storage secondary module): six-hours travel from one shelter to another one or to a point of interest (without stopping for surface operations).

For both cases, the energy and power peaks required from the module, result to be respectively 6.49 kWh and 6.49 kW.

4.4.2 Choice of the batteries

Given the short duration of the mission, it is proposed to furnish all the energy required by the module through power storage systems only, avoiding hazardous energy generation systems. In this sense, electrochemical batteries are the most widely used systems, and they can be primary or secondary [45], [46].

Rechargeable Lithium-Ion (Li-Ion) secondary batteries to be charged inside the shelters are chosen for the module over Regenerative Fuel Cells (RCFs), given their superior performances and Technology Readiness Level (TRL) [46],[47]. Furthermore, they are already being used for orbital missions, Mars rovers, and astronaut tools .

4.4.3 Proposed configuration of the power subsystem

The proposal of the configuration of the power subsystem is constituted of three rechargeable Li-Ion batteries:

- Two of them are already charged at the beginning of the journey and are dimensioned to furnish all the power needed by the different subsystems of the module; the two batteries are independent, so that, if only one of them is involved in an accident, the other will not be affected by it and will continue to give power to the connected loads.
- One of them is connected to and charged by the photovoltaic cells and can be used: a) in emergencies, in case one of the principal batteries fails, or b) as a principal battery for a subsequent mission.

The batteries are located outside the lower portion of the central body of the module, to minimize the loads burdening on the structure. From it, cables are directed to a DC/DC converter depart, to reduce the tension of the furnished energy. From the DC/DC converter, a wiring system distributes the electrical energy to all the subsystems and elements of the module that require power.

4.4.4 Dimensioning of the batteries

The Li-Ion cells considered for the analysis (LP 33450–43Ah, LP 33330–6Ah, LP 33037–60Ah) derive from EaglePicher Technologies.

The procedure exploited to derive the number of series and parallel cells that constitute the battery to fulfill the energy requirements (6.49 kWh per hour, with an additional margin of 25%) is adapted from [45], using the parameters summarized in *Table 10*:

Table 10. Batteries sizing parameters

Parameter	Value
Bus Voltage (V_{bus})	270 V [46]
Fade	0.013%/cycle
Depth of Discharge (DOD)	80%
Maximum Discharged Energy ($E_{max,\ discharge}$)	24375 Wh

From *Table 11*, it emerges that the typology of cells that allows the most efficient trade-off between mass and volume required is LP 33037 – 60Ah Space Cell. Therefore, this cell is selected among the proposed ones for the module.

Table 11. Results of the dimensioning of a single battery

	LP 33450 – 43Ah	LP 33330 – 6Ah	LP 33037 – 60Ah
N_s	75	75	75
N_p	3	3	16
Mass [kg]	285.75	360	316.35
Volume [dm^3]	0.5	0.66	0.1

4.4.5 Choice and dimensioning of the photovoltaic panels

Even though rechargeable batteries are used as the principal source of energy for the module, also photovoltaic (PV) panels to be installed on the external surface of the module are considered as secondary/emergency sources of energy.

The main features of the selected PV cells considered for the analysis are summarized in *Table 12*.

Table 12. Technical specification of PV cells

	CTJ30	IMM-α	CTJ30 - Thin	Z4J	UTJ32
Area [cm^2]	26.5	27.5	26.5	27.5	26.6
Efficiency	0.29	0.32	0.29	0.30	0.281
Mass [mg/cm^2]	85	49	50	-	84

Similarly to the sizing of the batteries, the procedure exploited to calculate the PV cells area needed to fulfill half of the total peak power required by the module in the most consuming scenario (3244 W, with an additional safety margin of 25%) is adapted from [50], using the parameters summarized in *Table 13*:

Table 13. PV cells sizing parameters

Parameter	Value
Irradiance (I)	1316 W/m^2 [49]
Inherent Degradation coefficient (I_d)	0.770 [50]
Sun incidence angle (θ)	10°
Degradation rate	2.5%/year (average value between 2-3% [44])
Service life	5 years

Among the proposed PV cells, IMM-α is chosen, since it provides the highest efficiency, with a comparable area to the others and a substantially lower mass.

The results of the dimensioning are the following: total area of 14.4 m^2 and total mass of 7 kg. The PV cells are used to recharge a third Li-Ion battery.

5. Module Design

5.1 Interior design

The internal configuration of the primary mobile module is defined by its main functions and therefore organized in three sectors: the cockpit, the center and the back.

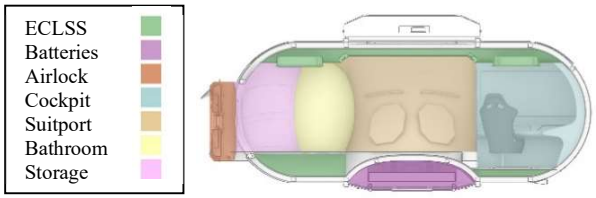

Fig. 11. Empty section of the module showing the functions with colors

The cockpit is dedicated to navigation and control, hosting wide desks with displays, speakers, projectors, and sensors. The shifting chairs on rails allow both the astronauts to reach all the controlling areas and to position themselves in front of the transparent surface of the shell which enables the drivers to look outside to the Moon's surface and the environment.

In the central body of the module, the suitport enables EVA explorations. The technology, originally patented in 1989 by M. Cohen, allows the astronaut to get in and get out of the space suit through a bulkhead opening keeping it on the outside of the pressurized habitat. This system has been selected for its advantages in terms of time reduction of preparation for EVA, airlock consumables, and its capacity to avoid contamination between the outside and the inside of the module [51].

Finally, two more seats for the crew members who are not driving, integrating storage boxes, are located in the back of the primary module. Furthermore, a circular bathroom is present, together with an equipped wall to store the tools for maintenance, the medical kit, food and cleaning tools, personal items, and the inventory management system. An airlock is present to connect the

primary module with other ones guaranteeing a continuous pressurized space.
ECLSS is essential to guarantee the environmental wellbeing of the astronauts: fans, heat pumps, sorption beds and filtering systems are located on the ceiling, while water tanks to store clean water, the one for recovery of the exhausted water and the oxygen and nitrogen tanks are stored under the flooring.
The power supply constituted by the batteries is located on the bottom, outside of the module.

Fig. 12. Render of the interior of the module

6. Conclusions

In this paper, a detailed study on a mobile space architecture system that enables human presence on the Moon during medium to long-term missions has been carried out.

After a preliminary research phase in which needs and requirements were identified, focusing on the mobile habitat and its subsystems, some analysis on the project's feasibility were conducted. The goal is to assure efficient structural support, proper mobility and speed for long-distance travel on the lunar surface, energy self-sufficiency over multiple conditions, and shielding for different hazards, besides a proposition of landing site analysis.

Two key concepts were used as reference for an unique solution: the "wagon train" – as the primary mobile module is in charge of navigation, followed through computer vision by the secondary modules – and the biophilic approach – as the modules' functional distribution is inspired by the bee's body, with the head containing navigation and communication systems, the torax with life-sustaining, energy and locomotion ones, and the abdomen representing the specific function of the secondary module selected for the mission.

On a technical matter, this research sought to find avant-garde materials for componing the module's design, as well as utilizing computational analysis performed with Grasshopper© and NASA's software OLTARIS © to assure a safe and efficient solution.

The multidisciplinary approach utilized to tackle the problem allows for a holistic viewpoint, but further research is encouraged for each of the subtopics.

Acknowledgments

The team wants to acknowledge Alta Scuola Politecnica, Thales Alenia Space, and MIT for the partnership that enabled the development of this project.

References

[1] ISECG Global Exploration Map Supplement, 28 August 2020, https://www.globalspaceexploration.org/wp-content/uploads/2020/08/GER 2020 supplement.pdf (accessed 28.07.22).
[2] S. Zhang et al., First measurements of the radiation dose on the lunar surface, Sciences Advances 39 (2020) 1-6.
[3] O. Bannova, L. Bell, Radiation shielding strategies for lunar minimal functionality habitability element, Acta Astronautica 67(2010) 1103-1109.
[4] National Aeronautics and Space Administration (NASA), Space Radiation, https://www.nasa.gov/hrp/elements/radiation (accessed 05.10.2021)
[5] E. Vanzani, V., Marzari, F., Dotto, Micrometeoroid Impacts on the Lunar Surface, 28th Annual Lunar and Planetary Science Conference, Houston, Texas, 1997, 17-21 March.
[6] E. L. Christiansen, D.M Lear, Micrometeoroid and Orbital Debris Environment & Hypervelocity Shields (2012).
[7] T. Y. Park, J. J. Lee, J. H. Kim, and H. U. Oh, Preliminary thermal design and analysis of lunar lander for night survival, Int. J. Aerosp. Eng (2018).
[8] B. Dubnar, Moon's South Pole in NASA's Landing Sites, 19 April 2019 https://www.nasa.gov/feature/moon-s-south-pole-in-nasa-s-landing-sites (accessed on 23.08.2022)
[9] G. Landis, Laser Power Beaming for Lunar Polar Exploration, 2020, doi: 10.2514/6.2020-3538.
[10] M. M. Cohen, and R. A. Tisdale, Habot Mobile Lunar Base Configuration Analysis, Space 2006, AIAA 2006-7335, San Jose, California, 2006
[11] D. Spenneberg, and F. Kirchner, The Bio-Inspired SCORPION Robot: Design, Control & Lessons Learned, Climbing and Walking Robots: towards New Applications, Houxiang Zhang (Ed.), InTech, 2007.
[12] Toyota Jaxa – Hydrogen Fuelled Lunar Vehicles https://www.toyota-europe.com/world-of-toyota/articles-news-events/2019/toyota-jaxa (accessed 29.11.2021)
[13] R. M. Boyle, K. Mitchell, C. Allton, and H. Ju, Suitport Feasibility – Development and Test of a Suitport and Space

Suit for Human Pressurized Space Suit Donning Tests, Lydon B. Johnson Space Center, National Aeronautics and Space Administration, Houston, Texas

[14] K. Robinson and D. Hitt, 'Space Launch System Artemis I CubeSats SmallSat Vanguards of Exploration, Science and Technology', SSC20-S2-05, 32nd Annual AIAA/USU Conference on Small Satellites, Utah, USA, 2018, 4-9 Aug

[15] E. Wallace, 'AIAA 93-0993 Considerations for the Design of Lunar Rover Structures and Mechanisms for Prolonged operation in the lunar environment, Aerospace Design Conference, 1993, Irvine, CA, 16-19 Feb

[16] S. K. Padisala, A. Bhardwaj, K. Poluri, and A. K. Gupta, 'Effect of Constrained Groove Pressing on Mechanical Properties of Nitinol Alloy' IMECE2018-87295, International Mechanical Engineering Congress and Exposition 2018, Pittsburgh, Pennsylvania, USA, 9-15 Nov

[17] Grasshopper, Algorithmic Modelling for Rhino, https://www.grasshopper3d.com/ (Accessed 20.08.22)

[18] Welcome to Karamba 3D, https://manual.karamba3d.com/ (Accessed 04.05.22)

[19] H. Benaroya, 'Lunar habitats: A brief overview of issues and concepts', REACH, vol. 7–8, Dec. 2017, pp. 14–33

[20] P. Manda, A. Pathak, A. Mukhopadhyay, U. Chakkingal, and A. K. Singh, 'Ti-5Al-5Mo-5V-3Cr and similar Mo equivalent alloys: First principles calculations and experimental investigations', J. Appl. Res. Technol., vol. 15, no. 1, Feb. 2017, pp. 21–26

[21] Ph. Lequeu, K. P. Smith, and A. Daniélou, 'Aluminum-Copper-Lithium Alloy 2050 Developed for Medium to Thick Plate', J. Mater. Eng. Perform., vol. 19, no. 6 (2010), pp. 841–847,

[22] M. M. Lima and R. Monteiro, 'Characterisation and thermal behaviour of a borosilicate glass', Thermochimica Acta, 373 (2001), 69-74

[23] Suojun Li, Haibo Gao, and Zongquan Deng, 'Mobility performance evaluation of lunar rover and optimization of rocker-bogie suspension parameters', 2nd International Symposium on Systems and Control in Aerospace and Astronautics, 2008, Shenzhen, China, 10-12 Dec

[24] A. S. Howe and B. Sherwood, Eds., Out of This World: The New Field of Space Architecture. American Institute of Aeronautics and Astronautics, Reston, VA, 2009.

[25] Rhinoceros3D, https://www.rhino3d.com/it/ (Accessed 20.08.22)

[26] E. Dimas and D. Briassoulis, '3D geometric modelling based on NURBS: a review', Advances in Engineering Software, vol. 30, no. 9–11 (1999), pp. 741–751,

[27] J. Trunins, A. Curley, B. Osborne, Design of a Mars rover mobility system. JBIS - Journal of the British Interplanetary Society. 65 (2012) 87–97.

[28] D. Apostolopoulos (2020). Reconfigurable wheel-track for all-terrain mobility (U.S. Patent US20220161875A1)

[29] S. A. Padula (2016). Superelastic tire (Patent US10449804B1)

[30] G. Z. Arsequell, Research of shape memory alloy wheels for Mars rovers, 2021.

[31] D. S. Apostolopoulos, Analytical Configuration of Wheeled Robotic Locomotion, 2001.

[32] S. Laurenzi, G. de Zanet, M. G. Santonicola, Numerical investigation of radiation shielding properties of polyethylene-based nanocomposite materials in different space environments, Acta Astronaut. 170 (2020) 530–538.

[33] M. Naito et al., Investigation of shielding material properties for effective space radiation protection, Life Sci. Sp. Res. 26 (2020) 69–76.

[34] R. Destefanis et al., Space environment characterisation of Kevlar®: good for bullets, debris and radiation too, Univers. J. Aeronaut. Aerosp. Sci. 2 (2014) 80–113.

[35] DuPont, KEVLAR Aramid Fiber - Technical Guide, 2017.

[36] E. L. Christiansen, B. A. Davis, Heat-Cleaned Nextel in MMOD Shielding, 6099 First Int'l. Debris Conf., Sugar Land, Texas, 2019, 9-12 December.

[37] P. M. Sutheesh, A. Chollackal, Thermal performance of multilayer insulation: A review, IOP Conf. Ser. Mater. Sci. Eng. 396 (2018) 0–8.

[38] T. C. Slaba, A. M. Mcmullen, S. A. Thibeault, C. A. Sandridge, M. S. Clowdsley, S. R. Blattnig, OLTARIS : An Efficient Web-Based Tool for Analyzing Materials Exposed to Space Radiation, Proceedings of SPIE-The International Society for Optical Engineering, 2011, September.

[39] R. C. Singleterry et al., OLTARIS : On-line tool for the assessment of radiation in space, Acta Astronaut. 68 (2011) 1086–1097.

[40] NASA standards, Crew Health - NASA-STD-3001, 2022, vol. 1. pp. 1–67.

[41] K. Creel, J. Frampton, D. Honaker, K. McClure, M. Zeinali, Pressurized Lunar Rover (NASA) (1992).

[42] V. A. Virginia Polytechnic Institute, Pressurized Lunar Rover (Dual Hull) (1992).

[43] D. A. Petri, R. L. Cataldo, J. M. Bozek, Power system requirements and definition for lunar and Mars outposts - A review of the Space Exploration initiative's NASA 90 Day Study, Collect. Tech. Pap. - 4th Int. Energy Convers. Eng. Conf., San Diego, California, 2006, 26-29 June.

[44] R. L. Cataldo, J. M. Bozek, Power requirements for the first lunar outpost (FLO), Tenth Symp. Sp. Nucl. Power Propuls., Albuquerque, New Mexico, 1993, 10-14 January.

[45] A. Peressotti, Lunar Base: power generation and thermal control system design, 2018.

[46] A. Damiano et al., Batteries for Aerospace: A Brief Review, AEIT.2018.8577355, 110th Int. Annu. Conf. AEIT, Bari, Italy, 2018, 3-5 October.

[47] T. W. Kerslake, Electric Power System Technology Options for Lunar Surface Missions, NASA Tech. Reports (2005).

[48] T. B. Miller, Battery Applications for NASA's Missions - A Historical Perspective, ARPA-E Robust Afford. Next Gener. EV-Storage, Orlando, Florida, 2014, 28-29 January.

[49] A. Z. Ribah, S. Ramayanti, Power produced analysis of solar arrays in nadir pointing mode for low-earth equatorial micro-satellite conceptual design, IOP Conf. Ser. Earth Environ. Sci. 284 (2019).

[50] S. Aranya, T. E. Girish, Moon's Radiation Environment and Expected Performance of Solar Cells during Future Lunar Missions, IMRC 2008 Conference, Chongqing, China, 2008, 9-12 June.

[51] M. M. Cohen, Mobile Lunar and Planetary Bases, Advanced Project Branch, Space Project Division, NASA-Ames Research Center, AIAA 2003-6280, Long Beach, California, 2003, 23-25 September